Journal of Hazardous Materials Advances 21 (2026) 100948

Contents lists available at ScienceDirect

Journal of Hazardous Materials Advances

journal homepage: www.elsevier.com/locate/hazadv

Sustainable leaching of nickel and cobalt from asbestos waste using deep eutectic solvents: Kinetic modeling and recovery performance

Rustam Sharipov [a], Assel Dagubayeva [a,b,*], Galymzhan Maldybayev [a,b], Mohamad Nasir Mohamad Ibrahim [c], Omirserik Baigenzhenov [d,1,**], Tiancheng Mu [e]

[a] School of Materials Science and Green Technologies, Kazakh-British Technical University, 59 Tole bi St, Almaty 050000, Kazakhstan
[b] RSE National Center on Complex Processing of Mineral Raw Materials of the Republic of Kazakhstan, Almaty 050036, Kazakhstan
[c] Materials Technology Research Group (MaTReC), School of Chemical Sciences, Universiti Sains Malaysia, 11800 Minden, Penang , Malaysia
[d] Department of Metallurgy and Mineral Processing, Satbayev university, Almaty 050013, Kazakhstan
[e] School of Chemistry and Life Resources, Renmin University of China, Beijing 100872, China

ARTICLE INFO

Keywords:
Asbestos wastes
Deep eutectic solvents (DES)
Nickel and cobalt leaching
Recycling
Kinetic modeling

ABSTRACT

A sustainable hydrometallurgical route was developed for the selective recovery of nickel and cobalt from asbestos production waste using a novel deep eutectic solvent (DES) composed of ethylene glycol and hydroxylamine hydrochloride. Magnetic separation yielded a Ni–Co-enriched fraction with a 10–12-fold increase in target metal content relative to the raw waste, as confirmed by WD-XRF, SEM/EDS, and chemical analysis. Under optimized conditions (80 °C, 4 h, L/S = 4:1), leaching efficiencies of 72.4 % for Ni and 79.6 % for Co were achieved, while co-dissolution of Fe, Mg, and Si remained below 8 %, demonstrating exceptional selectivity. Kinetic analysis revealed a dual-control mechanism: the excellent fit to the Prout–Tompkins model ($R^2 > 0.99$) reflects autocatalytic, ligand-assisted surface reactions driven by Ni^{2+}/Co^{2+} coordination with DES components, whereas the low activation energies (15.73 kJ/mol for Ni, 13.68 kJ/mol for Co) and strong agreement with the Jander diffusion model indicate that mass transfer through the evolving porous residue governs the overall rate. Critically, ^{1}H NMR spectroscopy of the spent DES shows pronounced signal broadening and attenuation due to paramagnetic Ni^{2+}/Co^{2+} ions, providing direct, solution-phase evidence of metal - ligand complexation - a key advancement over indirect FTIR data alone. Complementary SEM and XRD analyses confirm selective phase dissolution without bulk matrix degradation. These results establish the DES as an environmentally benign, ligand-functionalized leaching medium that enables the valorization of hazardous asbestos waste into a secondary source of critical metals, aligning with green and circular hydrometallurgical principles.

Nickel is a silvery-white metal with a characteristic luster, known for its high corrosion resistance, ductility, and favorable mechanical properties (Kelamanov et al., 2024). It belongs to the group of transition metals and is characterized by a high melting point (1455 °C) as well as the ability to form stable alloys with numerous other elements. Due to these properties, nickel is widely used across various industries, including metallurgy, chemical manufacturing, electronics, energy, and battery production. One of the key applications of nickel is in the production of stainless steel, where it enhances the strength, corrosion resistance, and thermal stability of alloys (Abdirashit et al., 2025). In recent decades, the use of nickel in the production of lithium-ion batteries has gained particular importance (Kurmanbayeva et al., 2021), driven by the growing demand for electric vehicles and renewable energy sources. Additionally, nickel is used in catalysts (Massenova et al., 2020), specialized coatings (Assylbekova et al., 2023; Osipov et al., 2025), coinage (Gavrilă et al., 2024), and the aerospace industry (Smith et al., 2001).

The primary sources of nickel are sulfide and laterite ores (Ivanov et al., 2022). Sulfide ores are characterized by a relatively high nickel content and favorable beneficiation conditions, making them particularly attractive for industrial processing. These ores are typically located at significant depths and require underground mining; however, they

* Corresponding author at: School of Materials Science and Green Technologies, Kazakh-British Technical University, 59 Tole bi St, Almaty 050000, Kazakhstan.
** Corresponding author.
E-mail addresses: a_dagubayeva@kbtu.kz (A. Dagubayeva), o.baigenzhenov@satbayev.university (O. Baigenzhenov).
[1] Department of Metallurgy and Mineral Processing, Satbayev university, Almaty 050013, Kazakhstan.

https://doi.org/10.1016/j.hazadv.2025.100948
Received 24 July 2025; Received in revised form 2 October 2025; Accepted 19 November 2025
Available online 20 November 2025

offer consistent raw material quality and high metal recovery rates. In contrast, laterite ores are formed through intense weathering of ultramafic rocks under tropical climatic conditions. In such ores, nickel is predominantly present in the form of oxides and hydroxides, necessitating the use of different technological approaches for its extraction. Nickel ore processing methods include pyrometallurgical and hydrometallurgical techniques, with the choice depending on the mineral composition of the raw material, technological capabilities, and economic feasibility (Moskalyk and Alfantazi, 2002). Under conditions of sustained growth in nickel demand-particularly driven by the advancement of battery technologies and the transition to a low-carbon economy - the annual depletion of traditional nickel ore reserves is becoming increasingly significant. This necessitates the active search for alternative sources of metal that can provide a stable raw material supply for industry while simultaneously reducing environmental impact. One promising direction is the utilization of industrial waste containing nickel as a secondary raw material. Such waste includes:

- Electroplating sludges, generated during nickel plating processes, which may contain up to 5–15 % Ni depending on the technology and operating conditions (Liu et al., 2023);
- Fly ash from the combustion of coal and other fuels, which contains nickel in the range of 0.01–0.3 % Ni (Izquierdo and Querol, 2012);
- Metallurgical slags, especially those from the processing of nickel and copper-nickel ores, which may contain 0.1–2.5 % Ni (Kelamanov et al., 2021).

Among these nickel-bearing industrial wastes, asbestos tailings generated during the mining and processing of serpentinite rocks are of particular interest (Baigenzhenov et al., 2022). These anthropogenic deposits, accumulated in volumes estimated at millions of tons, contain nickel concentrations of up to 0.4 %, which is comparable to low-grade laterite ores. Moreover, they also contain cobalt, opening up opportunities for integrated processing to recover multiple valuable components. Thus, asbestos tailings can be considered a strategically important reserve source of nickel and cobalt, especially in the context of the shift toward resource-efficient and environmentally sustainable technologies.

As is well known, in Kazakhstan, the processing of chrysotile asbestos ore yields only 6–8 % of marketable fiber from the total volume of extracted rock. The remaining mass over 92 % - is classified as waste and is not utilized further (Baigenzhenov et al., 2015). Over >60 years of mining and beneficiation of serpentinite ores, substantial volumes of industrial waste have accumulated, with a total mass exceeding 300 million tons. These wastes represent a potentially valuable secondary resource, as they contain nickel concentrations of 0.2–0.4 %, equivalent to 600–1200 thousand tons of metal, and cobalt concentrations of 0.08–0.12 % (i.e., 240–360 thousand tons). One of the key advantages of processing these industrial materials is their surface location and pre-crushed state, which eliminates the need for mining operations. This significantly reduces the cost of extracting valuable components and enhances the economic attractiveness of processing. The efficiency and profitability of technologies aimed at processing already extracted and crushed materials have been confirmed by a number of scientific studies. However, most of these studies have focused primarily on magnesium recovery and the production of its compounds, such as magnesium sulfate and chloride. Meanwhile, the potential of asbestos waste as a source of nickel and cobalt remains insufficiently explored, despite their significant concentrations in these anthropogenic deposits. This highlights the need for further research aimed at developing integrated technologies that enable the efficient recovery of all valuable components.

It is important to note that the utilization of chrysotile asbestos production waste not only enables the recovery of valuable components but also addresses significant environmental challenges (Baigenzhenov et al., 2024). Finely ground waste, stored on the surface for extended periods, is subject to weathering, resulting in the dispersion of fine particles into the surrounding environment. These particles naturally settle on the soil surface, forming dense deposits of varying thickness, which contribute to land degradation and the development of soil erosion processes.

An additional factor contributing to the formation of dense surface deposits is the presence of calcium oxides in the waste. When interacting with atmospheric precipitation (rain and snow), calcium promotes the formation of cement-like crusts on the ground in areas where the waste settles. These compacted asbestos-based formations reduce soil permeability and hinder vegetation growth, which, in the long term, may lead to further land degradation. Such processes have already been observed across extensive areas surrounding waste storage sites, within a radius of up to 50 km. Of particular concern is the impact of asbestos-containing particles on human health. Fine chrysotile fibers suspended in the air can penetrate the respiratory system and accumulate in the lungs, causing severe diseases such as silicosis and silicotuberculosis. Therefore, the processing of chrysotile asbestos industrial waste represents not only an economically viable but also an environmentally significant approach that contributes to reducing the technogenic burden on the environment and improving the ecological situation in adjacent regions (Shayakhmetova et al., 2024; Macher et al., 2025).

In order to improve the environmental performance of the studied technology, it was decided to explore the use of deep eutectic solvents (DESs) as leaching agents. In recent years, these compounds have attracted growing scientific interest as a promising alternative to traditional acidic reagents in hydrometallurgical processes (Zante and Boltoeva, 2020; Deblonde et al., 2022). Due to their low toxicity, minimal impact on equipment, and selective interaction with metal ions, DESs are considered environmentally friendly reagents for the extraction of base and rare metals. Their physicochemical properties -particularly thermal stability and low volatility - ensure resilience across a wide temperature range, making them especially promising for leaching nickel and cobalt from both mineral and anthropogenic sources. One such anthropogenic source is chrysotile asbestos production waste, which has accumulated over decades and contains significant amounts of nickel and cobalt. However, as previously noted, the extraction of these metals from such waste has received insufficient attention to date. Most existing studies have focused primarily on magnesium recovery, mainly in the form of chloride and sulfate salts, while the potential of these wastes as a source of non-ferrous metals has remained largely untapped (Chu et al., 2025).

In this context, the present study explores the possibility of extracting nickel and cobalt from asbestos-containing waste using deep eutectic solvents. This approach aims to bridge the existing scientific and technological gap while enhancing the synergistic indicators of environmental sustainability and resource efficiency. The use of DESs not only enables the processing of previously unused industrial waste but also aligns with the principles of green chemistry, minimizing environmental impact and reducing technological costs.

1. Materials and methods

1.1. Sample collection and characterization

In this study, asbestos production waste generated during the manufacturing of asbestos fibers was selected as the raw material for the recovery of valuable metal components. Upon collection, the bulk material was dried in an electric furnace at 95 °C for 4 h to remove residual moisture. The dried waste was then subjected to grinding in a ball mill to reduce particle size and ensure homogeneity. Subsequent sieving was carried out using a standard mesh to isolate the <0.25 mm fraction, which was further processed by magnetic separation under a magnetic field strength of 1500 Oersted. This procedure yielded a magnetic fraction accounting for approximately 5.0–5.2 % of the initial mass.

1.2. Analytical techniques

All sample mass measurements were conducted using a high-precision analytical balance (RA214C, Ohaus-Pioneer) with a readability of ±0.0005 g. Deionized water used for rinsing the solid residues after leaching was obtained from a Milli-Q purification system (Millipore), providing a resistivity of 18.2 MΩ·cm. The elemental composition of the magnetic fraction was determined by wavelength-dispersive X-ray fluorescence (WD-XRF) using an Axios spectrometer (PANalytical). The phase composition of both the enriched magnetic fractions and the leach residues was characterized by X-ray diffraction (XRD) using a D8 Advance diffractometer (Bruker). Microstructural and surface morphology analysis of the magnetic fraction was carried out using a JEOL JXA-8230 electron probe microanalyzer (JEOL, Akishima, Tokyo, Japan). Elemental distribution mapping was performed with the integrated energy-dispersive X-ray (EDX) spectrometer to visualize the spatial distribution of key elements. Furthermore, Fourier-transform infrared (FTIR) spectroscopy (Bruker) was employed to analyze the changes in functional groups and chemical bonding in the DES before and after leaching. ^{1}H NMR spectra of the pristine and spent DES were recorded at 25 °C on a Bruker Avance III 400 MHz spectrometer using acetone-d_6 as the solvent. Quantitative determination of nickel and cobalt concentrations in the DES leachates was performed using an atomic absorption spectrometer (TAS 990).

1.3. Preparation of deep eutectic solvents

Ethylene glycol (99.8 %) and hydroxylamine hydrochloride (99.0 %) were purchased from Sigma-Aldrich and used without further purification. The reagents were mixed in a 4:1 ratio and stirred at 60 °C for 1 h to obtain a homogeneous and translucent $NH_2OH{\cdot}HCl$/EG solution. The synthesized DES was subsequently analyzed by FTIR spectroscopy (Fig. 3) and transferred into leaching vessels for further experimental investigations.

1.4. Leaching procedure

The leaching experiments were carried out using a controlled batch method. A 20 g sample of the Ni-Co-bearing magnetic fraction was introduced into a sealed glass reactor equipped with a mechanical agitator and a sampling port. The reaction temperature was precisely regulated using a thermostatic bath with an accuracy of ±1 °C. Prior to initiating the leaching process, both the solid waste material and the (DES) were independently preheated to the target temperature - the solid phase inside the reactor and the DES in a separate flask.

Upon reaching thermal equilibrium, the preheated DES was promptly added to the reactor containing the solid sample, thereby initiating the leaching process. Stirring began immediately upon addition of the solvent, and this moment marked the start of the experimental time. Liquid samples (aliquots) were withdrawn at predetermined intervals of 60, 120, 180, and 240 min for subsequent analysis. All experiments were performed in triplicate to ensure reproducibility, and the resulting data were averaged. Laboratory glassware was rigorously cleaned with ultrapure deionized water prior to each experiment. At each sampling interval, a 5.0 mL aliquot of the leachate was collected via the sampling port and diluted to a final volume of 250 mL. The concentrations of nickel and cobalt in the diluted solutions were determined using atomic absorption spectroscopy

The leaching efficiency (LE) of Ni and Co was calculated as the percentage of the total mass of each metal extracted into solution relative to its initial content in the solid sample, using the following equation:

$$LE\ (\%) = \frac{C_A \cdot V}{C_{in} \cdot M} 100 \quad (1)$$

Where: C_A (gL^{-1}) is the concentration of Ni and Co in the samples (leach liquor); V (L) is the leach liquor volume; C_{in} is the Ni and Co content in the asbestos wastes; and M (g) is the mass of the Ni and Co.

The influence of key operational parameters on Ni and Co leaching efficiency was systematically investigated. The studied parameters included temperature, leaching duration, and liquid-to-solid (L/S) ratio. Following each leaching experiment, the productive nickel- and cobalt-containing DES solution was separated from the solid phase by centrifugation. Subsequently, the solid residue was rinsed twice with distilled water to remove residual leaching agent and dried in an oven at 95 °C for 4 h.

2. Kinetic regularities of the leaching process

Leaching kinetics represents a key aspect in the study and optimization of hydrometallurgical processes, as it enables the quantitative description of metal dissolution rates and the identification of rate-limiting steps related to mass transfer and chemical interactions (Yessengaziyev et al., 2025). Depending on the physicochemical properties of the system and the operational conditions, the leaching process may be controlled by reagent diffusion through a boundary layer, by a surface chemical reaction on the solid phase, or by diffusion through a layer of the reaction product. A profound understanding of kinetic patterns provides the ability to predict system behavior under varying process parameters and serves as a foundation for developing more efficient and environmentally sustainable metal extraction methods. To gain deeper insight into the kinetic characteristics, leaching must be considered as a sequence of consecutive stages, each of which may exert a dominant influence on the overall reaction rate (Tokpayev et al., 2025).

At the molecular level, leaching involves the transport of reagents from the bulk solution to the solid surface, penetration of the solvent through a porous structure or the layer of reaction products, chemical interaction at the phase boundary, and diffusion of the reaction products back into the solution. To identify which particular stage governs the overall leaching process, several classical kinetic models are employed, including the Jander, Drozdov–Rotinyan, Prout–Tompkins, and shrinking core model.

2.1. Essence and equation of the Jander model

The Jander equation is one of the earliest models used to describe diffusion-controlled reactions in spherical particles. It assumes that the reaction occurs at the interface between the unreacted core and the product layer, and the rate is limited by the diffusion of reactants through this growing product shell (Ray and Ray, 2018).

$$\left[1-(1-\alpha)^{1/3}\right]^2 = kt \quad (2)$$

α - recovery degree, (%);

τ- is the duration of interaction, (min);

k - reaction rate constant, (is a proportionality constant for a given reaction), (min^{-1});

The model implies that as the reaction proceeds, a dense, non-porous product layer forms around the unreacted core, and ions must diffuse through this layer to sustain the reaction. It is applicable when internal diffusion through this product layer governs the rate, typical of many silicate and oxide minerals.

2.2. Essence and equation of the Drozdov–Rotinyan model

This model was developed to account for both diffusion and chemical resistance, including the slowing down of reaction rate due to the accumulation of secondary products that may partially block reactive surfaces or pores.

$$\frac{1}{\tau}\ln\left(\frac{1}{1-\alpha}\right) - \beta\frac{\alpha}{\tau} = M \quad (3)$$

α - recovery degree, (%);
τ- is the duration of interaction, (min);
β and M − are the coefficients of braking and total speed, respectively.

The left-hand side of the equation includes both a term for reaction kinetics and a «braking» term that captures the deceleration of leaching over time. This model is particularly relevant when leaching proceeds initially fast but becomes slower due to the formation of passivating layers or changes in solid morphology (Baigenzhenov et al., 2024).

2.3. Essence and equation of the Prout–Tompkins model

The Prout–Tompkins model is often used for processes characterized by autocatalytic behavior or where nucleation and growth phenomena play a significant role. It is especially suited to S-shaped (sigmoidal) kinetic curves.

$$ln\left(\frac{\alpha}{1-\alpha}\right) = kln\tau + b \quad (4)$$

α - recovery degree, (%);
k- reaction rate constant (is a proportionality constant for a given reaction), (min^{-1});
τ- is the time, (min);
b- is a rate constant that describes the rate at which solutes are transferred from one medium to another.

This model suggests that the reaction rate increases as the product forms, possibly due to enhanced surface area or autocatalysis, and then declines as reactants are depleted. It is used when leaching does not follow simple first- or zero-order kinetics but instead involves intermediate activation stages (Brown, 1997).

2.4. The activation energy

Activation energy (Ea) is a fundamental thermodynamic parameter that characterizes the minimum energy required for a chemical reaction to occur. In the context of leaching processes, Ea represents the energy barrier that reacting species must overcome at the solid–liquid interface in order to form reaction products. The magnitude of the activation energy provides insight into the nature of the rate-limiting step of the process:

- at low activation energy values (typically <20 kJ/mol), the process is generally controlled by mass transfer mechanisms, such as external or internal diffusion (Nadirov et al., 2020);
- at high values (<40 kJ/mol), the surface chemical reaction becomes the rate-limiting step.

Quantitatively, the relationship between the reaction rate and temperature is described by the Arrhenius equation:

$$k = A_{exp}\left(-\frac{E_a}{RT}\right) \quad (5)$$

A_{exp} - is the frequency factor;
E_a– is the apparent activation energy, (kJ/mol);
R- is gas equilibrium constant, R = 8.314 (J/mol);
T- is the absolute temperature, (K).

3. Results and discussion

3.1. Characterization of the magnetic fraction and the deep eutectic solvent

Prior to leaching, the magnetic fraction obtained via dry magnetic separation was thoroughly characterized to evaluate its potential as a feedstock for selective Ni and Co recovery. X-ray diffraction (XRD) analysis (Fig. 1) revealed a complex multiphase mineralogy dominated by iron oxides. The diffraction pattern is consistent with the coexistence of magnetite (Fe_3O_4) and hematite (Fe_2O_3), indicating the presence of both Fe^{2+} and Fe^{3+} oxidation states.

Additional reflections were indexed to magnesioferrite ($MgFe_2O_4$) and a nickel-bearing spinel phase, tentatively assigned to $NiFe_2O_4$. The incorporation of Mg^{2+} and Ni^{2+} into the spinel lattice - most likely via isomorphous substitution - confirms that nickel is structurally integrated within the oxide matrix rather than occurring as a discrete, readily leachable phase.

Scanning electron microscopy (SEM) imaging (Fig. 2) displayed angular, irregularly shaped particles with a heterogeneous surface morphology and dispersed fine inclusions - features characteristic of high-energy ball milling followed by magnetic separation. Compositional analysis by energy-dispersive X-ray spectroscopy (EDS) of a representative particle yielded the following elemental distribution (wt. %): Fe – 45.31, Mg – 8.90, Si – 3.69, Ni – 2.38, and Co – 0.32, underscoring a pronounced enrichment in the target metals relative to the raw asbestos waste.

Quantitative oxide composition was further determined by wavelength-dispersive X-ray fluorescence. The magnetic fraction was found to consist of approximately 76.2 wt.% Fe_3O_4, 9.9 wt.% MgO, 9.7 wt.% SiO_2, 2.67 wt.% NiO, 0.17 wt.% CoO, and 1.36 wt.% Cr_2O_3, in excellent agreement with XRD and SEM/EDS data. Critically, this represents a 10–15-fold enrichment in Ni and Co compared to the untreated waste (which typically contains 0.18–0.24 wt.% Ni and 0.02–0.04 wt.% Co), with EDS confirming final concentrations of 2.98 wt.% Ni and 1.39 wt.% Co. These results validate dry magnetic separation as a highly effective pre-concentration strategy for Ni–Co-bearing phases in asbestos tailings. In parallel, the deep eutectic solvent (DES), synthesized from ethylene glycol (EG) and hydroxylamine hydrochloride ($NH_2OH{\cdot}HCl$) in a 4:1 molar ratio, was characterized by Fourier-transform infrared (FTIR) spectroscopy (Fig. 3).

The spectrum is dominated by a broad and intense absorption band centred at ~3178 cm^{-1}, significantly red-shifted from the typical O–H/N–H stretching region of free hydroxyl or amine groups (~3400–3500 cm^{-1}). This shift provides compelling evidence of extensive intermolecular hydrogen bonding between the hydroxyl groups of EG and the protonated amine functionality of NH_3^+OH. The absence of sharp, component-specific vibrational modes - coupled with the emergence of new bands at 1448 cm^{-1} (C–H bending) and 1144 cm^{-1} (C–O–H deformation) - confirms the formation of a homogeneous, hydrogen-bonded eutectic network. Additional diagnostic features include C–H stretches at 2930 and 2875 cm^{-1}, an H–O–H bending mode at 1628 cm^{-1} (suggesting trace water), and a series of C–O/C–N stretching vibrations between 1200 and 900 cm^{-1}, consistent with strong donor–acceptor interactions between EG and $NH_2OH{\cdot}HCl$. Collectively, these spectral signatures corroborate the successful synthesis of a stable, ligand-rich DES capable of coordinating transition metal ions - thereby establishing its suitability as a tailored leaching medium for Ni and Co extraction. The observed features align closely with established DES systems reported in the literature (Smith et al., 2014; Abbott et al., 2004; Othman et al., 2015).

To further corroborate the molecular structure and hydrogen-bonding network of the as-prepared DES, ^{1}H NMR spectroscopy was employed. The spectrum of the pristine $NH_2OH{\cdot}HCl$/ethylene glycol (4:1) DES (Fig. 4) exhibits two dominant resonances: a broad signal centered at 6.28 ppm (integral ≈ 1.92), assigned to the hydroxyl (–OH) protons of ethylene glycol engaged in strong hydrogen bonding with the protonated amine group ($–NH_3^+$) of hydroxylamine hydrochloride, and a sharper multiplet at 3.56 ppm (integral ≈ 1.08), corresponding to the methylene ($–CH_2–$) protons.

The pronounced downfield shift of the –OH resonance - by >2.5 ppm relative to free ethylene glycol ($\delta \approx 3.6$ ppm) - provides direct evidence of extensive intermolecular hydrogen bonding between the hydrogen

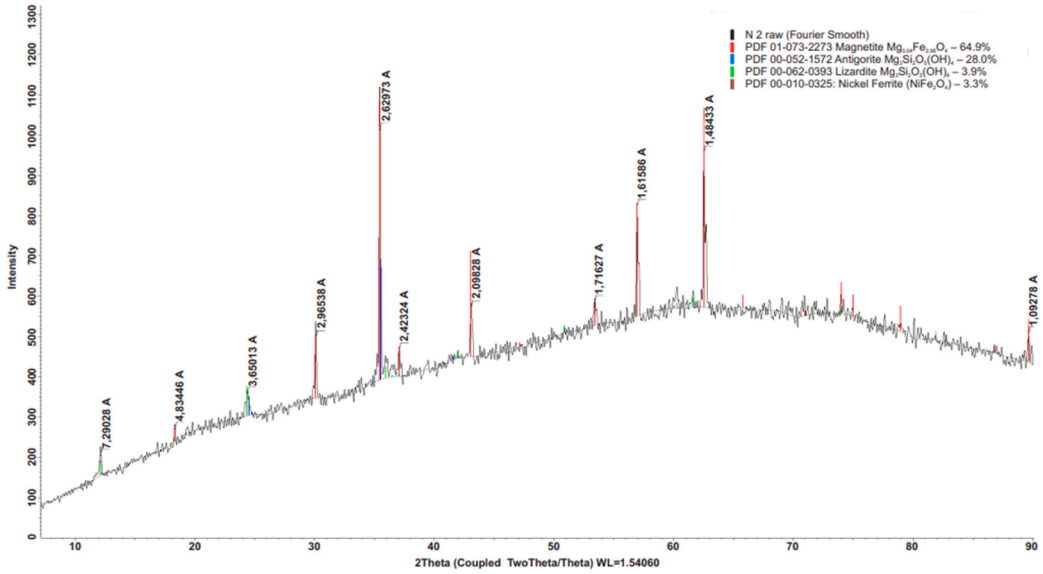

Fig. 1. The XRD pattern of the magnetic fraction.

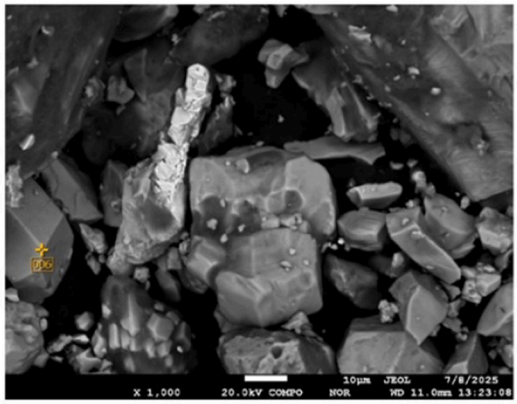

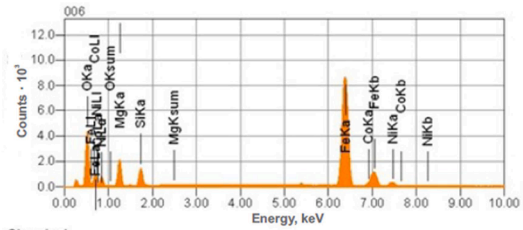

Chemical

formula	ms%	mol%	Sigma	Net	K ratio	Line
O	17.32	39.40	0.11	954236	0.1030058	K
Mg	5.94	8.90	0.14	553151	0.0160822	K
Si	2.85	3.69	0.11	414253	0.0132287	K
Fe	69.52	45.31	0.30	5009223	0.5531946	K
Co*	0.53	0.32	0.39	31183	0.0040902	K
Ni	3.85	2.38	0.51	178044	0.0284065	K
Total	100.00	100.00				

Fig. 2. SEM micrograph and corresponding EDX spectrum of the magnetic fraction.

bond donor (NH_3^+OH) and acceptor (EG) components. This observation is fully consistent with the FTIR data and confirms the formation of a homogeneous, thermally stable eutectic liquid with a high density of potential coordination sites, thereby reinforcing its capacity to act as a selective ligand-based leaching medium for transition metals.

3.2. *The effects of leaching temperature and time*

Temperature is one of the key parameters exerting a significant influence on the efficiency of leaching processes. An increase in temperature generally accelerates chemical reactions, enhances the solubility of both reagents and reaction products, and promotes the breakdown of the crystalline lattice of ore minerals, thereby facilitating the access of the leaching agent to target components. However, higher temperatures do not always lead to improved leaching performance. For example, in atmospheric acid leaching of nickel and cobalt sulfide ores, it has been observed that temperatures above 90 °C can lead to the formation of passivating layers of sulfur and jarosite on the surface of mineral particles. These layers hinder further interaction between the reagent and the ore, ultimately reducing metal recovery. Similarly, in high-temperature pressure leaching of lateritic ores, operating at temperatures above 250 °C may result in the formation of poorly soluble iron and aluminum sulfates, which are capable of sorbing nickel and cobalt, thus decreasing their extraction efficiency. These examples underscore the importance of selecting an optimal temperature regime that accounts for phase transformations and chemical interactions within the system (Mamyrbayeva et al., 2024).

In our study, leaching experiments were carried out in the temperature range of 20 to 80 °C (Fig. 5). This range was selected to evaluate the kinetic behavior of the process under conditions close to those encountered in industrial practice. According to the experimental results, increasing the leaching temperature from 20 to 80 °C led to a significant improvement in the extraction of nickel (from 16.5 to 72.4 %) and cobalt (from 27.8 to 79.6 %). A similar trend was observed when extending the leaching duration from 60 to 240 min at 80 °C: the nickel extraction increased from 21.6 to 72.4 %, and cobalt from 24.3 to 79.6 %. This behavior is attributed not only to the intensification of chemical interactions between DES components and metal ions, but also to a pronounced decrease in solvent viscosity at elevated temperatures. The reduced viscosity enhances mass transfer and promotes deeper penetration of the solvent into the porous structure of the leached material (Abbott et al., 2004).

The deep eutectic solvent (DES) used in this study exhibits strong ligand properties due to the presence of hydroxylamine, which is capable of forming stable coordination complexes with Ni^{2+} and Co^{2+} ions. Hydroxylamine can act as an electron donor and participate in the formation of chelating structures, thereby enhancing the solubility of metals. Moreover, protonated hydroxylamine ($NH_3OH^+Cl^-$), under

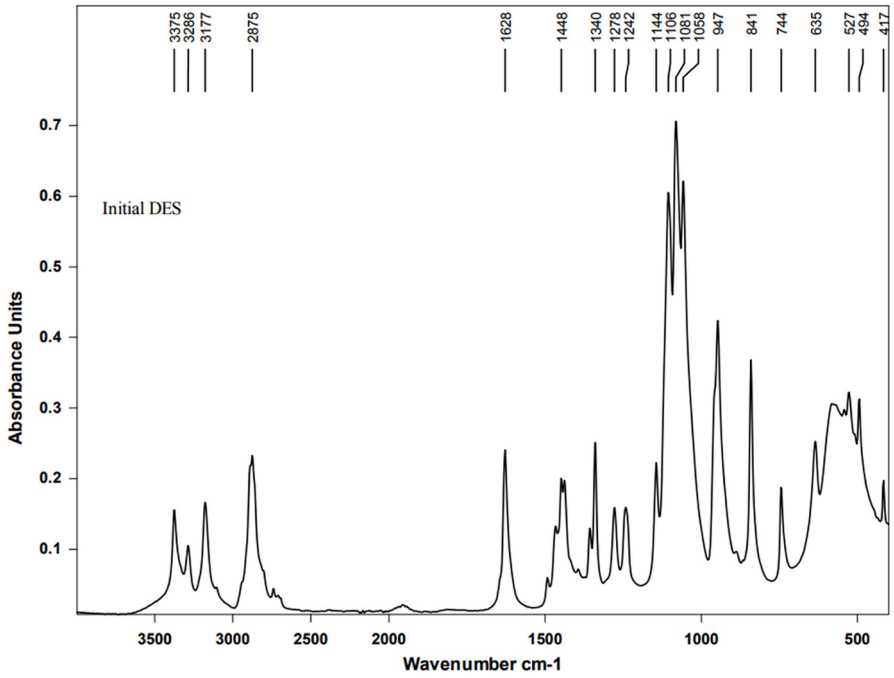

Fig. 3. FTIR spectrum of the initial deep eutectic solvent.

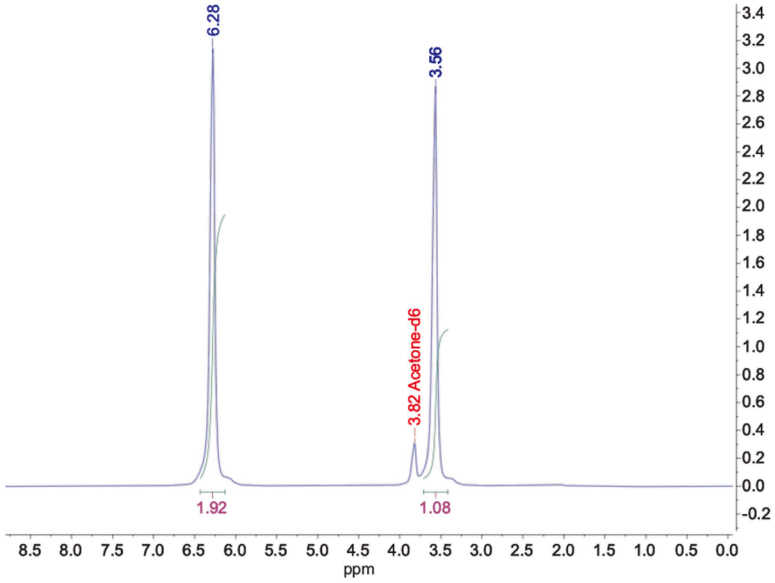

Fig. 4. ^{1}H NMR spectra of (a) pristine DES.

moderately acidic conditions (pH ~2–3), provides H^+ ions that facilitate the destruction of the silicate matrix of minerals containing nickel and cobalt (Delina et al., 2024).

The observed increase in metal recovery with prolonged treatment time at 80 °C confirms a transition of the system from a surface reaction-controlled regime to one governed by internal diffusion. In the initial stages, when active sites on the particle surface are readily available, the reaction between metal cations and DES components proceeds rapidly. The high selectivity of the DES toward Ni^{2+} and Co^{2+} - with >65 % extraction while Fe, Mg, and Si remain largely intact (<8 % loss) - results in a structurally modified solid phase rather than a classical passivating layer. As these surface sites become depleted, the process becomes increasingly limited by the diffusion of ions through the evolving porous residue, which acts as a diffusional barrier due to structural reorganization and partial matrix depletion (Fig. 6).

The high viscosity of the DES, combined with its complexation ability, slows down the outward migration of dissolved ions, which explains the deceleration of the leaching process at later stages (Smith et al., 2014).

Fig. 7 presents four flasks containing solutions obtained from the leaching of the nickel- and cobalt-bearing magnetic fraction of asbestos production waste at different temperatures: 20 °C, 40 °C, 60 °C, and 80 °C. Initially, the DES used as the leaching medium was transparent. However, after the leaching process, a distinct color change was observed in the solutions, indicating the extraction and transfer of metal ions into the liquid phase.

As the temperature increases, a notable intensification in the colour of the solutions is observed: from light green at 20 °C to a deep, almost

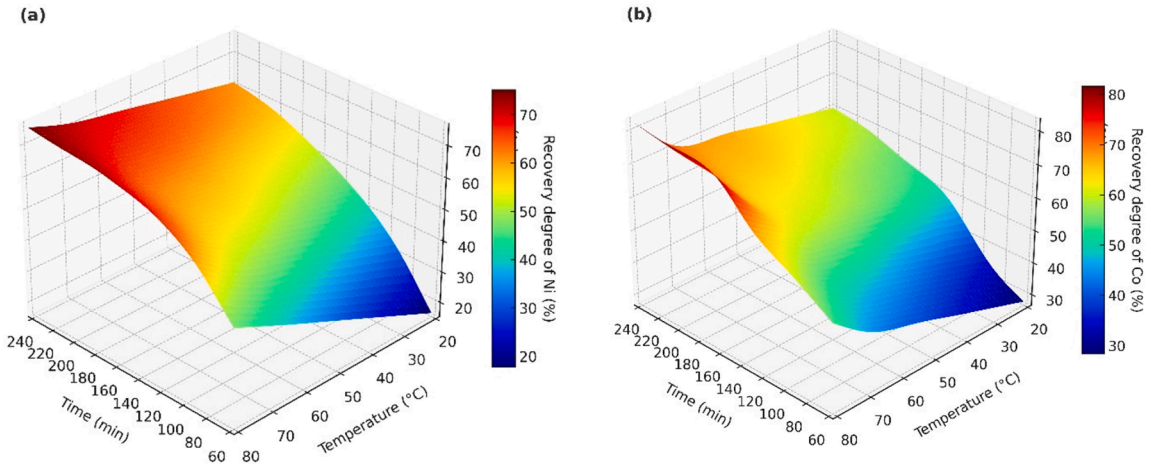

Fig. 5. 3D surface plots of the recovery efficiency of (a) Ni and (b) Co as a function of temperature and leaching time using deep eutectic solvent (DES) as leaching agent.

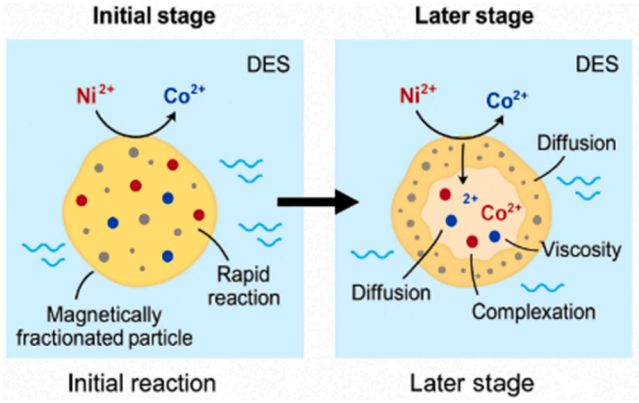

Fig. 6. Schematic illustration of the proposed leaching mechanism of Ni^{2+} and Co^{2+} using deep eutectic solvent (DES): rapid surface reaction at the initial stage followed by diffusion-controlled processes and complexation at the later stage.

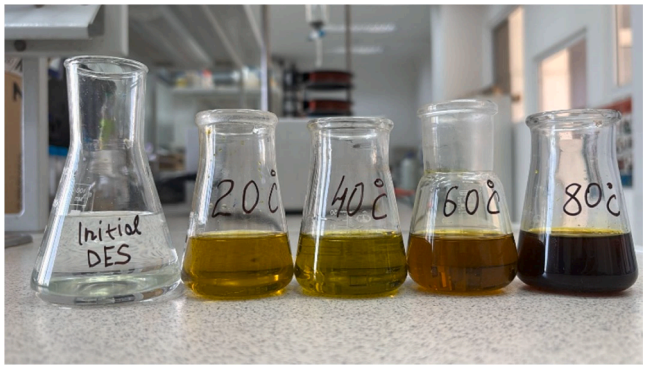

Fig. 7. Photographic comparison of DES leachates after magnetic fraction leaching at various temperatures.

black hue at 80 °C. This indicates a temperature-dependent increase in the extraction efficiency of target metals such as nickel and cobalt, which may be attributed to enhanced solubility and kinetic activity of the components at elevated temperatures.

3.3. Effect of liquid-to-solid phase ratio (L:S ratio)

The solid-to-liquid phase ratio (S:L) is one of the key parameters in leaching processes using deep eutectic solvents (DESs), as it significantly influences mass transfer efficiency and reagent availability within the system. DESs are generally characterized by higher viscosity compared to conventional inorganic acids, making them particularly sensitive to an excess of solid phase. When the liquid phase is insufficient, system hydrodynamics deteriorate, diffusion of reagents and products is restricted, and the risk of local saturation increases, potentially reducing the extraction efficiency of target metals.

Conversely, increasing the proportion of the liquid phase promotes more uniform distribution of the solvent, improves contact between the reagent and the mineral surface, and accelerates leaching kinetics. However, excessive dilution may lead to lower metal concentrations in the solution, increased volumes of circulating liquids, and consequently, higher costs for downstream processing. Therefore, selecting the optimal S:L ratio when using DESs requires a comprehensive approach, considering the physicochemical properties of the solvent, the characteristics of the ore material, and the technological conditions of the process.

As shown in Table 1, the effect of the liquid-to-solid phase ratio (L:S) ranging from 3:1 to 5:1 on the extraction efficiency of nickel and cobalt into the DES solution has been investigated in this study.. It was shown that increasing the L:S ratio from 3:1 to 4:1 led to an increase in nickel extraction from 66.5 to 72.4 %, and cobalt extraction from 71.3 to 79.6 %. Further increase to 5:1 had no significant effect, indicating that equilibrium and solvent saturation had been reached.

At a low liquid volume (3:1), mass transfer limitations and reduced activity of complexing agents may occur due to the insufficient amount of solvent for effective ion extraction. From a practical standpoint, the optimal ratio is 4:1, as it ensures high extraction efficiency while maintaining a moderate reagent consumption Table 1.

The obtained results are consistent with the literature data. For example, Calgaro et al. (Calgaro et al., 2015) investigated the efficiency of metal leaching from silicate ores using chloride-containing DESs, and demonstrated that at temperatures of 80–90 °C, nickel and cobalt extraction rates of 70–75 % could be achieved. However, in their case, pre-enriched ore with a lower specific surface area was used, which explains the somewhat slower kinetics. Smith et al. (2014) and Hartley

Table 1
Effect of liquid-to-solid phase ratio on the leaching efficiency of Ni and Co.

liquid-to-solid phase ratio	recovery degree, %	
	Ni	Co
3:1	66.5	71.3
4:1	72.4	79.6
5:1	72.4	79.6

et al. (2014) emphasized the role of chloride ions as coordinating agents in DES systems, particularly in the presence of additional ligands such as hydroxylamine, which enhance metal solubility and stabilization in solution.

3.4. Selectivity of Ni and Co leaching and phase transformations in the residue

The claim of selective recovery of nickel and cobalt from asbestos waste using the ethylene glycol–hydroxylamine hydrochloride (DES) is substantiated by a direct comparison of the elemental composition and microstructure of the solid phase before and after leaching, complemented by spectroscopic analysis of the spent solvent. Energy-dispersive X-ray spectroscopy (EDS) of the magnetic fraction prior to leaching (Fig. 2) revealed the following elemental composition (in wt. %): Fe – 45.31, Mg – 8.90, Si – 3.69, Ni – 2.38, and Co – 0.32. After leaching under optimized conditions (80 °C, 4 h, L:S = 4:1), the residue exhibited a dramatic reduction in nickel content - to 0.80 wt.% - corresponding to the extraction of approximately 66 % of the initial Ni. Cobalt showed a similar trend, with its concentration decreasing from 0.32 wt.% to 0.11 wt.%, indicating a removal of over 65 %. In stark contrast, the major matrix elements - Fe, Mg, and Si - underwent only marginal changes. The Fe content decreased from 45.31 wt.% to 42.1 wt. %, representing a relative reduction of just ~7 %. Given that the total mass of the solid residue also decreased due to metal extraction, this minor shift implies that <7 % of the total iron inventory was transferred into solution. Similarly, magnesium declined only slightly from 8.90 wt. % to 8.2 wt.% (a ~8 % relative decrease), while silicon decreased from 3.69 wt.% to 3.4 wt.% (~8 % relative loss). These minimal changes stand in sharp contrast to the >65 % extraction of Ni and Co and provide compelling evidence of the DES's high selectivity toward the target metals over the dominant Fe–Mg–Si oxide-silicate matrix.

Scanning electron microscopy (Fig. 8) further supports this interpretation. The leached residue displays a significantly altered morphology compared to the dense, compact particles of the feed material (Fig. 2): the surface becomes porous, fractured, and etched, indicative of localized, non-uniform dissolution rather than bulk matrix degradation. This morphological transformation aligns with the chemical data and suggests that the DES selectively targets sites hosting labile Ni^{2+} and Co^{2+} ions - most likely substituting for Mg^{2+} in the spinel structure of magnesioferrite ($MgFe_2O_4$) - while leaving the Fe-rich oxide and silicate framework largely intact. The persistence of Fe-, Mg-, and Si-rich domains in the residue, as confirmed by EDS elemental mapping (Fig. 8), underscores the stability of the host matrix under the applied leaching conditions.

FTIR spectroscopy of the DES before (Fig. 3) and after leaching (Fig. 9) offers molecular-level insight into the coordination mechanisms underpinning the observed selectivity. The post-leaching spectrum exhibits a marked attenuation of the broad O–H/N–H stretching band in the 3300–3175 cm^{-1} region, signifying active participation of hydroxyl and amino functional groups in metal coordination. Concurrently, new vibrational features emerge at 1453 cm^{-1} and within the 1030–500 cm^{-1} range - specifically at 1031, 1007, 878, 681, and 512 cm^{-1} - consistent with deformation modes and M–O stretching vibrations characteristic of metal–ligand complexes.

Critically, given the minimal depletion of Fe, Mg, and Si in the solid residue (as quantified by EDS - <8 % relative loss), the spectral alterations in the spent DES are predominantly ascribed to the formation of Ni–O and Co–O coordination bonds with DES constituents. This assignment is chemically reasonable: hydroxylamine (NH_2OH), present in equilibrium with its protonated form NH_3OH^+ under the mildly acidic conditions of the DES (pH ≈ 2–3), acts as an N,O-bidentate ligand capable of chelating transition metal ions. Ethylene glycol (EG) further contributes as a neutral O-donor ligand through its hydroxyl and ether oxygen atoms. The resulting mixed-ligand environment selectively stabilizes Ni^{2+} and Co^{2+} - which readily form labile, soluble complexes

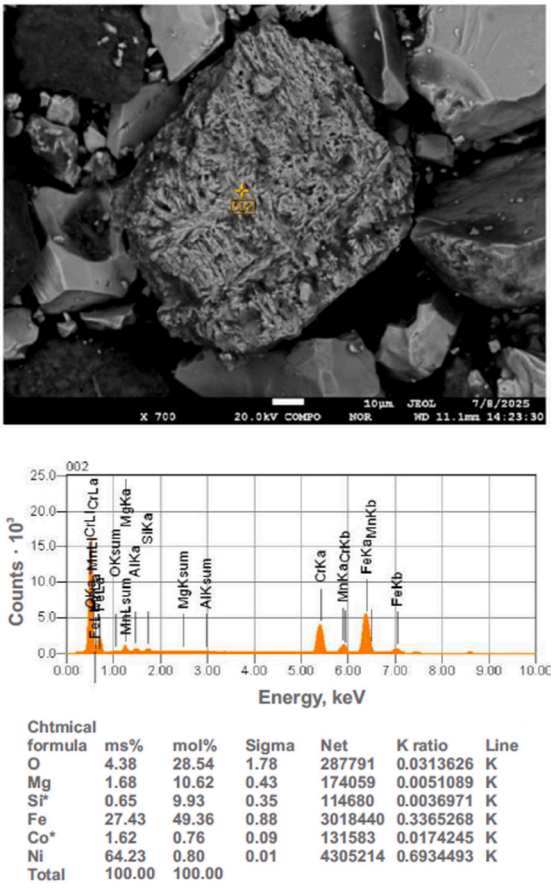

Chtmical formula	ms%	mol%	Sigma	Net	K ratio	Line
O	4.38	28.54	1.78	287791	0.0313626	K
Mg	1.68	10.62	0.43	174059	0.0051089	K
Si*	0.65	9.93	0.35	114680	0.0036971	K
Fe	27.43	49.36	0.88	3018440	0.3365268	K
Co*	1.62	0.76	0.09	131583	0.0174245	K
Ni	64.23	0.80	0.01	4305214	0.6934493	K
Total	100.00	100.00				

Fig. 8. SEM image, EDX spectrum, and elemental composition of the magnetic fraction after leaching.

with N/O-donor ligands - while Fe^{3+}, Mg^{2+}, and Si^{4+} remain largely uncomplexed due to their lower affinity for such ligands under these conditions. The FTIR band attenuation at 3300–3175 cm^{-1} (O–H/N–H stretch) and the emergence of features at 1453 cm^{-1} (deformation modes) and 1031–512 cm^{-1} (M–O stretches) thus provide direct spectroscopic evidence for coordination-driven leaching of Ni and Co, rather than non-selective acidolysis. This assignment aligns with the well-documented affinity of hydroxylamine for Ni^{2+} and Co^{2+}, which promotes their selective solubilization through stable complexation, while less labile Fe^{3+}, Mg^{2+}, and Si^{4+} remain structurally integrated within the residual oxide-silicate matrix.

Complementing the FTIR findings, ^1H NMR analysis of the spent DES (Fig. 10) offers direct, solution-phase evidence of metal–ligand coordination through characteristic paramagnetic effects. Upon comparison with the pristine DES spectrum, the post-leaching sample exhibits dramatic changes: the broad –OH resonance shifts upfield to 4.89 ppm and becomes significantly broader and less intense, while the $–CH_2–$ signal shifts slightly downfield to 3.80 ppm and also displays pronounced line broadening. Most critically, the overall signal intensity is markedly attenuated. These spectral alterations - particularly the severe peak broadening and signal quenching - are hallmark signatures of interactions between proton nuclei and paramagnetic metal ions such as Ni^{2+}, Co^{2+}, and possibly Fe^{2+}/Fe^{3+}.

In NMR spectroscopy, paramagnetic centers induce rapid transverse relaxation (T_2 shortening), which broadens or even suppresses resonances of nuclei in close spatial proximity. The observed effects thus confirm that the oxygen atoms of ethylene glycol and the nitrogen/oxygen donors of hydroxylamine are in direct coordination with dissolved transition metal ions, forming paramagnetic complexes in solution. This constitutes direct spectroscopic proof of a ligand-assisted leaching

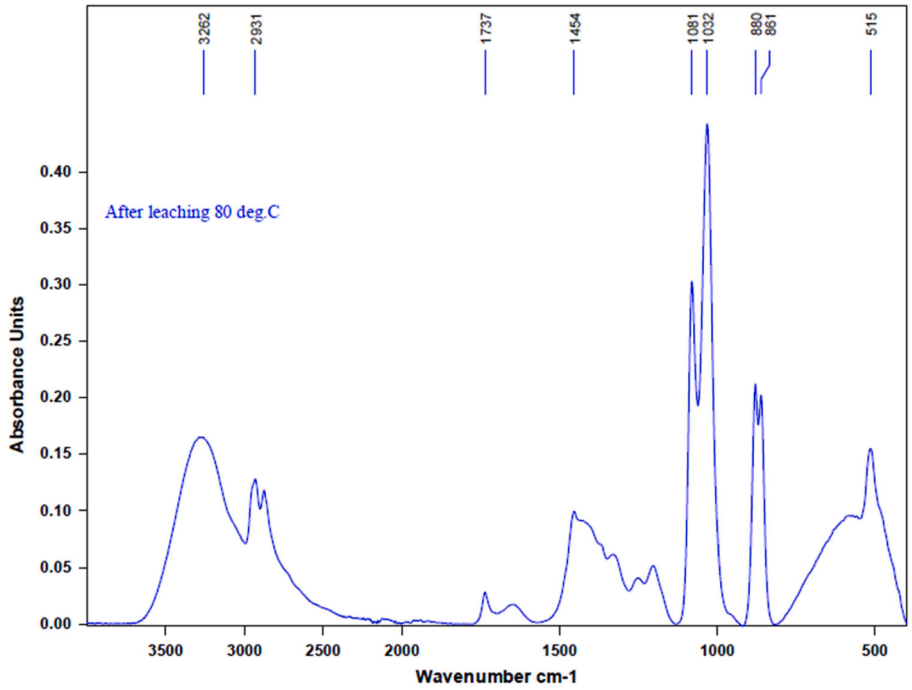

Fig. 9. FTIR spectrum of the deep eutectic solvent (DES) after leaching of the magnetic fraction.

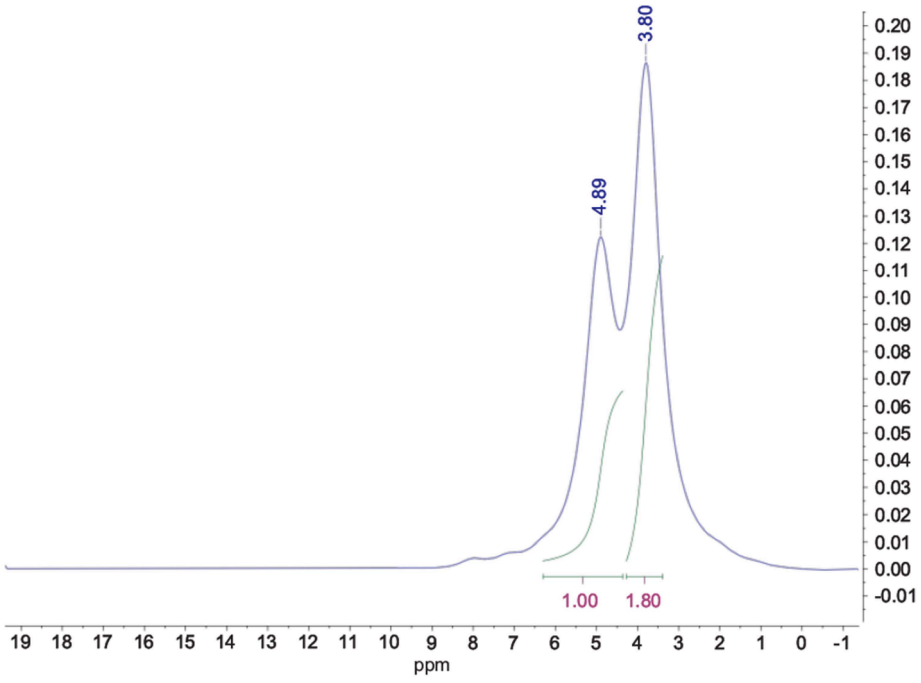

Fig. 10. ^{1}H NMR spectra of spent DES after leaching under optimized conditions (80 °C, 4 h, L/S = 4:1).

mechanism, going beyond the indirect functional-group evidence provided by FTIR. The combined FTIR and NMR data therefore establish a consistent molecular picture: the DES selectively extracts Ni and Co not through bulk acid attack, but via the formation of soluble, paramagnetic coordination complexes stabilized by mixed O/N-donor ligands - precisely the behavior expected from a tailored, green leaching system. Together, the EDS, SEM, and FTIR data collectively demonstrate that leaching proceeds not via non-selective acidolysis or bulk matrix disintegration, but through a ligand-driven, site-specific extraction of structurally vulnerable Ni and Co ions. The Fe–Mg–Si framework remains largely intact, as evidenced by the marginal compositional shifts (<8 % relative loss for Fe, Mg, and Si) and the preservation of particle morphology in non-reactive domains. This high degree of selectivity - exceeding 65 % extraction for both Ni and Co while suppressing co-dissolution of major matrix elements - is a decisive advantage for downstream separation and purification. Moreover, the FTIR spectrum of the spent DES reveals no signs of thermal or chemical degradation, confirming the solvent's robustness at 80 °C over extended reaction times. This stability underscores its potential for regeneration and reuse in closed-loop hydrometallurgical cycles, thereby enhancing both the

economic viability and environmental sustainability of the process.

While the term «sustainable» is often invoked in the context of deep eutectic solvents, its validity must be substantiated through direct comparison with conventional hydrometallurgical reagents. In this regard, the present DES system offers distinct environmental and process advantages over mineral acids such as H_2SO_4 or HCl when applied to complex silicate matrices like asbestos waste. Conventional acid leaching of such materials typically requires elevated temperatures (≥90 °C), high liquid-to-solid ratios (L/S ≥ 10:1), and generates large volumes of acidic effluents laden with Fe, Mg, and Si due to non-selective matrix dissolution (Baigenzhenov et al., 2015; Shayakhmetova et al., 2024). This necessitates costly downstream neutralization, sludge handling, and metal separation steps, significantly increasing the environmental footprint. In contrast, the $NH_2OH{\cdot}HCl$/ethylene glycol DES operates effectively at 80 °C and a low L/S ratio of 4:1, achieving 72.4 % Ni and 79.6 % Co recovery while suppressing co-dissolution of Fe, Mg, and Si to <8 %. This high selectivity eliminates the need for extensive neutralization and reduces secondary waste generation by orders of magnitude. Moreover, both components of the DES - ethylene glycol and hydroxylamine hydrochloride - are biodegradable, non-volatile, and exhibit low ecotoxicity compared to corrosive, volatile mineral acids (Smith et al., 2014). The absence of chloride or sulfate anions also avoids the formation of stable metal salts that complicate recovery and pose disposal challenges. From an energy perspective, the mild operating temperature (well below the boiling point of ethylene glycol, 197 °C) enables atmospheric-pressure operation using standard equipment, avoiding the energy-intensive pressurized systems often required for acid leaching of refractory silicates. Taken together, these attributes - reduced reagent consumption, minimal waste generation, inherent safety, and lower energy demand - provide a robust basis for describing the proposed process as environmentally benign and aligned with the principles of green chemistry.

To contextualize the performance of the developed $NH_2OH{\cdot}HCl$/EG DES system, Table 2 compares Ni and Co leaching efficiencies reported in recent literature using various DES formulations. Notably, the referenced studies often employed significantly higher liquid-to-solid (L/S) ratios - such as 20:1 in Ketegenov et al. (2024) and 10:1 in Zante and Boltoeva (2020) - resulting in substantially more diluted leachates. In contrast, the present work achieves competitive or superior extraction yields (72.4 % Ni, 79.6 % Co) at a much lower L/S ratio of 4:1, which enhances metal concentration in the pregnant leach solution and reduces downstream processing costs.

This low solvent consumption in our work aligns directly with the principles of green chemistry - specifically, waste minimization and process intensification - by reducing reagent usage, energy demand, and the volume of secondary effluents. The efficiency is particularly significant given that the feedstock - magnetic fraction of asbestos waste - is a complex, low-grade secondary resource with structurally bound Ni and Co, unlike the more reactive battery materials or pre-treated ores used in comparative studies.

4. Comparative fitness of the kinetic models

Based on the results of kinetic modeling of nickel and cobalt leaching from the magnetic fraction of asbestos-containing waste in a DES medium, a comprehensive evaluation was conducted regarding the applicability of classical kinetic models, including the Jander diffusion equation, the Drozdov–Rotinyan model, and the Prout–Tompkins equation. The aim of this analysis was not only to identify the rate-limiting step, but also to gain a deeper understanding of the interaction mechanism between the solid phase and the leaching solution, grounded in the fundamental principles of chemical kinetics, diffusion, and interfacial mass transfer theory. The selection of the Jander, Drozdov–Rotinyan, and Prout–Tompkins models was motivated by their ability to capture distinct physical features expected in this complex leaching system:

(i) the Jander model accounts for diffusion through a growing porous product layer, consistent with the residue morphology observed by SEM;
(ii) the Drozdov–Rotinyan model addresses kinetic deceleration due to pore blockage or passivation, which may occur as the silicate matrix partially dissolves; and
(iii) the Prout–Tompkins model describes autocatalytic behavior, which is plausible given the ligand-rich nature of the DES and the potential for metal–ligand complexation to enhance dissolution. Therefore, all three mechanisms were considered a priori and tested comparatively.

The Jander model was found to be the simplest and most physically interpretable among those used. For nickel, approximation of the experimental data yielded the equation $y = 0.0016x + 0.4718$ with a coefficient of determination $R^2 = 0.9555$, while for cobalt the equation was $y = 0.0017x + 0.4826$ with $R^2 = 0.9597$ (Fig. 11). The high R^2 values, close to unity, indicate a strong agreement between the model and the experimental data. This suggests that the process kinetics are controlled by internal diffusion through the solid residue layer formed on the particle surface during leaching.

The higher slope of the regression line for cobalt may be attributed to its greater chemical mobility within the residue structure and its higher tendency to form complexes with DES components, which reduces activation energy and accelerates mass transfer. The similar y-intercepts for both metals indicate comparable initial leaching conditions, confirming the similarity of their mineral forms. This supports the conclusion that DES effectively interacts with both nickel- and cobalt-bearing phases, enabling a predominantly diffusion-controlled leaching mechanism.

According to Fick's law, the rate of mass transfer is proportional to the concentration gradient, and the process slows down as the diffusion layer thickness increases - a trend that was observed in the present study. Similar diffusion-controlled leaching processes involving non-ferrous metals using ionic liquids and DESs have previously been described in several studies, including Tian et al. (2010).

When the data were processed using the Drozdov-Rotinyan model, the resulting linear relationships were less pronounced. For nickel, the approximation yielded the equation $y = –0.1584x + 0.0047$ with a coefficient of determination $R^2 = 0.0641$, indicating a lack of linear correlation and, therefore, poor suitability of this model for describing the process. For cobalt, the equation $y = 1.1085x + 0.0003$ with $R^2 = 0.8473$ demonstrated a moderate degree of fit, suggesting that the model

Table 2
Comparison of Ni and Co recovery efficiencies achieved with various deep eutectic solvents (DESs) from different feedstocks.

Feedstock	DES composition	L/S ratio (ml/g)	T, (°C)	Time, h	Ni recovery (%)	Co recovery (%)	Reference
Asbestos waste (this work)	$NH_2OH{\cdot}HCl$ / Ethylene glycol (1:4)	4:1	80	4	72.4	79.6	This study
Spent Li-ion batteries	ChCl / Oxalic acid	20:1	90	2	94.1	95.3	Ketegenov et al. (2024) (Ketegenov et al., 2024)
Laterite ore	ChCl / Citric acid	10:1	100	6	68.2	71.5	Zante and Boltoeva (2020) (Zante and Boltoeva, 2020)

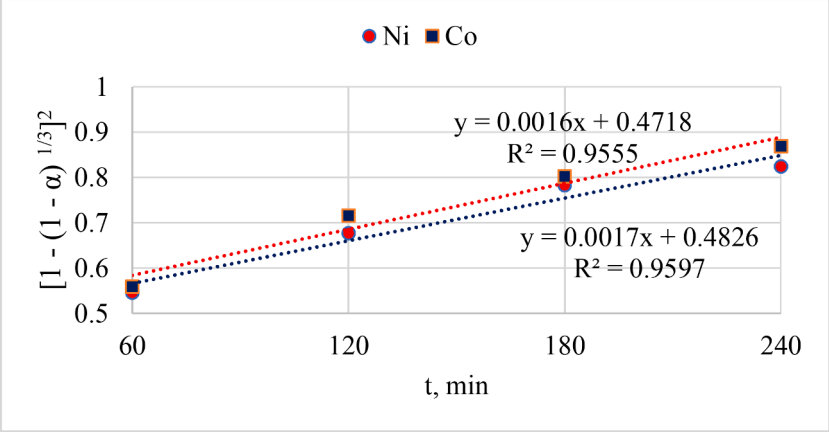

Fig. 11. Linearized form of the Jander model, plotted as $[1-(1-\alpha)^{1/3}]^2$ versus time.

may be conditionally applicable for cobalt only (Fig. 12).

The positive slope coefficient observed for cobalt, in contrast to the negative value for nickel, indicates a difference in the dissolution mechanisms of the two metals. It can be assumed that the leaching kinetics of nickel are more strongly influenced by side processes, such as passivation, gel-like structure formation, or competitive interactions with DES components - factors not accounted for by this model. Moreover, the low R^2 value for nickel may result from a violation of the model's assumptions, which are based on the autocatalytic nature of dissolution - a scenario that is unlikely under diffusion-controlled conditions.

The kinetic analysis of the leaching process using the Prout–Tompkins equation demonstrated an almost perfect correlation between experimental data and theoretical predictions. The linearized kinetic plots yielded equations of the form $y = 1.6616x - 8.0775$ ($R^2 = 0.9961$) for nickel and $y = 1.7821x - 8.4214$ ($R^2 = 0.9987$) for cobalt, respectively (Fig. 13). The exceptionally high coefficients of determination indicate the outstanding adequacy of this model in describing the ongoing process under the experimental conditions. Notably, the slope values exceeding unity −1.6616 for nickel and 1.7821 for cobalt - can be interpreted as indicative of autocatalytic effects or process activation by intermediate reaction products. According to the principles of chemical kinetics, particularly the law of reaction rate and chain reactions, such behavior suggests that the products of the reaction may enhance the reactivity of the system, either by destabilizing the residual mineral matrix or by activating the leaching agent via intermediate complex formation.

In the context of deep eutectic solvents (DESs), such autocatalytic behavior may arise from the formation of transient metal-ligand complexes involving solvent components such as ethylene glycol or hydroxylamine hydrochloride ions. These complexes may enhance the solubilization of metal ions by increasing the effective reactivity of the leaching environment. Similar mechanisms were reported by González-Gallardo et al. (2024), who observed that autocatalytic and coordinative interactions between metal ions and DES constituents accelerated the dissolution of metal species in high-viscosity ionic media.

Moreover, the greater slope observed for cobalt compared to nickel suggests that cobalt leaching is more sensitive to time-dependent changes in the system, which may reflect a more dynamic mass transfer regime and a higher degree of complexation Cimpoesu and Ferbinteanu (2018) . This difference is likely rooted in the distinct coordination chemistry of Co^{2+} and Ni^{2+} ions in DES media. Cobalt ions possess a higher tendency to form labile and kinetically favorable coordination complexes with donor atoms (such as oxygen and nitrogen centers) present in the solvent matrix. This has been corroborated by spectroscopic studies, including FTIR and NMR analyses, as described in the works of Abbott et al. (2004), which demonstrated pronounced solvation and coordination behavior of cobalt in various hydrogen bond donor–acceptor systems. Recent studies further support the relevance of autocatalytic and ligand-driven mechanisms in DES-based leaching systems. For instance, a competitive coordination strategy in a ternary DES was shown to simultaneously enhance leaching kinetics and enable selective precipitation of nickel oxalate from spent battery cathodes by

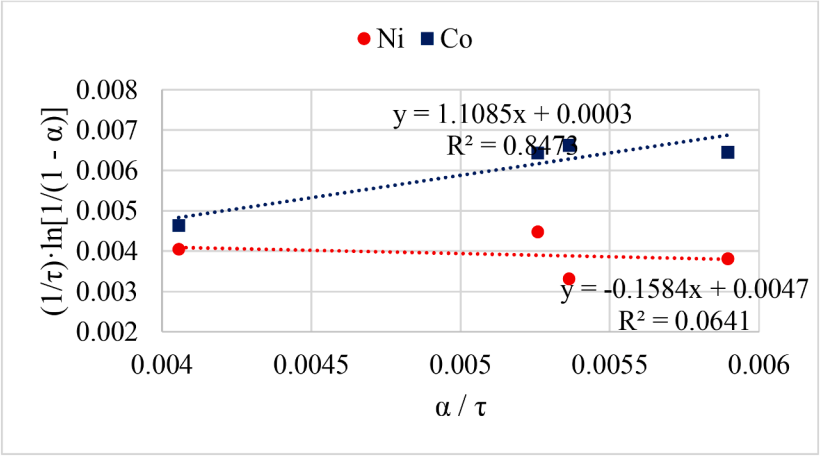

Fig. 12. Linearized form of the Drozdov-Rotinyan model, plotted as $(1/\tau)\cdot\ln[1/(1-\alpha)]$ versus α/τ.

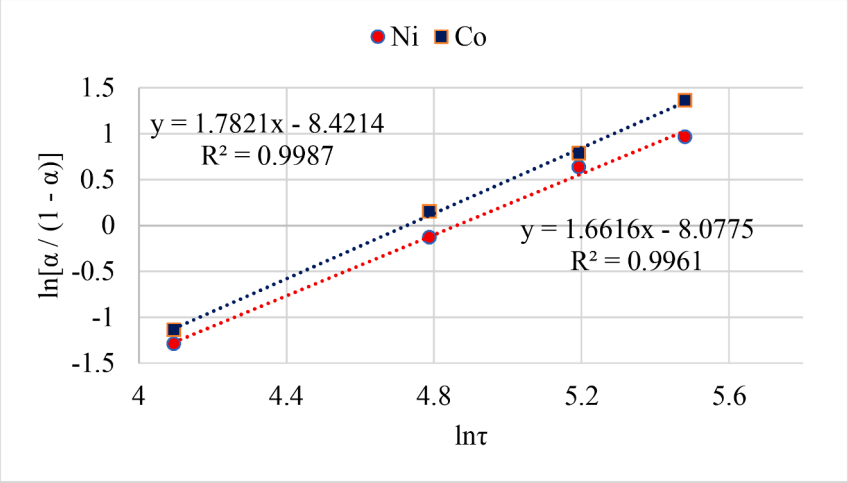

Fig. 13. Linearized form of the Prout–Tompkins model, plotted as ln[α/(1−α)] versus lnτ.

modulating nanostructure solvation shells (Tan et al., 2024). This underscores the broader applicability of ligand-assisted, autocatalytic pathways in complex DES media - consistent with the Prout–Tompkins behavior observed in our system.

The excellent agreement between experimental data and the Prout-Tompkins kinetic model, as discussed above, highlights the complexity and multistage nature of the leaching process in deep eutectic solvent systems. The observed kinetic behavior, particularly the high slope values and the linearity of transformation plots, supports the hypothesis that the process is governed not only by surface reactions or mass transfer limitations but also by chemical transformations influenced by coordination and intermediate formation. However, while the Prout–Tompkins model provides insights into the autocatalytic features and temporal dynamics of the process, a deeper understanding of the thermally activated nature of metal dissolution requires an evaluation of the temperature dependence of the leaching rate.

To further elucidate the influence of temperature on the leaching kinetics and to determine the energy barrier associated with the dissolution of nickel and cobalt, the Arrhenius equation was employed. For cobalt, the resulting linear equation was $y = -1.6456x + 5.1368$, with a coefficient of determination $R^2 = 0.9870$, while for nickel, the equation took the form $y = -1.8919x + 5.6697$, with $R^2 = 0.9792$ (Fig. 14).

The obtained activation energy values (13.68 kJ/mol for Co and 15.73 kJ/mol for Ni) fall within the range typically associated with diffusion-controlled processes (<20 kJ/mol), consistent with mass transfer limitations through the product layer or boundary layer (Nadirov et al., 2020). This observation aligns with the good fit of the Jander model ($R^2 > 0.95$), which assumes diffusion through a growing product shell as the rate-limiting step. However, the even better correlation with the Prout–Tompkins model ($R^2 > 0.99$) suggests that the leaching mechanism is not purely diffusive but involves autocatalytic surface reactions that accelerate metal dissolution once initial

Table 3
Kinetic model fitting parameters for Ni and Co leaching using deep eutectic solvent: regression equations and correlation coefficients (R^2) for Jander, Drozdov–Rotinyan, Prout–Tompkins, and Arrhenius models.

Model	Metal	Equation	R^2
Jander	Ni	$y = 0.0016x + 0.4718$	0.9555
	Co	$y = 0.0017x + 0.4826$	0.9597
Drozdov–Rotinyan	Ni	$y = -0.1584x + 0.0047$	0.0641
	Co	$y = 1.1085x + 0.0003$	0.8473
Prout–Tompkins	Ni	$y = 1.6616x - 8.0775$	0.9961
	Co	$y = 1.7821x - 8.4214$	0.9987
Arrhenius	Ni	$y = -1.8919x + 5.6697$	0.9792
	Co	$y = -1.6456x + 5.1368$	0.987

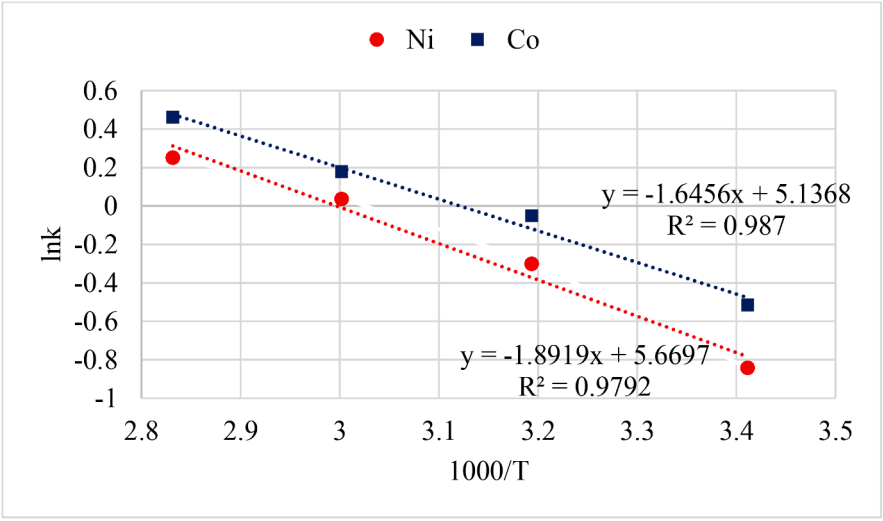

Fig. 14. Arrhenius plots for the leaching of Ni and Co.

complexes are formed. These R^2 values are summarized in Table 3, which compares the kinetic fitting parameters for all four models evaluated in this study. Thus, the process appears to be governed by a mixed mechanism, where diffusion through the evolving porous residue limits the overall rate, while surface coordination with DES ligands drives selectivity and enables autocatalytic enhancement Table 3.

Thus, the Arrhenius-based activation energy analysis complements the kinetic modeling, offering thermodynamic validation for the proposed multistage mechanism.

These findings demonstrate that the DES achieves selective extraction of nickel and cobalt not through aggressive acid dissolution of the entire mineral matrix, but via ligand-assisted, site-selective leaching of structurally labile transition metal ions. The Fe–Mg spinel framework remains largely intact, while Ni^{2+} and Co^{2+} - due to their favorable coordination chemistry with hydroxylamine and ethylene glycol - are efficiently complexed and solubilized as mixed-ligand cationic species of the type $[M(EG)_a(NH_2OH)_\beta]^{2+}$ (M = Ni, Co). This mechanism aligns with the autocatalytic kinetics described by the Prout–Tompkins model ($R^2 > 0.99$), indicating that surface coordination with DES ligands drives selectivity and enhances dissolution. However, the low activation energies (13.68 kJ/mol for Co and 15.73 kJ/mol for Ni) and the good fit of the Jander model confirm that the overall rate is limited by diffusion through the evolving porous residue. The demonstrated selectivity is a critical advantage for downstream purification and represents a significant step toward sustainable, low-impact valorization of hazardous asbestos waste.

5. Conclusion

The deep eutectic solvent system composed of ethylene glycol and hydroxylamine hydrochloride demonstrated high efficiency in extracting nickel and cobalt from the magnetic fraction of asbestos processing waste. Magnetic separation yielded a concentrate with a 10–12-fold enrichment in Ni and Co content compared to the original material, as confirmed by XRF, SEM/EDS, and chemical analysis. Leaching experiments conducted over a temperature range of 20–80 °C showed a strong positive correlation between temperature and metal extraction efficiency, achieving 72.4 % for nickel and 79.6 % for cobalt at the highest tested temperature.

Kinetic analysis was performed using the Jander, Drozdov–Rotinyan, and Prout–Tompkins equations. The Prout - Tompkins model exhibited the best correlation ($R^2 > 0.99$), indicating an autocatalytic surface reaction mechanism. Activation energy values of 15.73 kJ/mol for nickel and 13.68 kJ/mol for cobalt suggest that the leaching process is primarily controlled by diffusion through the product layer or boundary layer, consistent with mass transfer limitations.

FTIR spectroscopy of the DES after leaching revealed changes in vibrational modes associated with the formation of metal–ligand complexes. SEM and XRD analyses of the solid residues showed morphological and structural changes consistent with the partial removal of metal-bearing phases. The DES retained its chemical integrity after leaching, suggesting the possibility of reuse in subsequent cycles. These findings support the applicability of deep eutectic solvents as efficient and environmentally benign leaching agents for the recovery of valuable metals from industrial waste streams such as asbestos processing residues.

From a practical and sustainable process design perspective, the optimal leaching conditions are identified as 80 °C, 4 h, and a liquid-to-solid ratio of 4:1 (mL/g). These parameters deliver high recovery efficiencies (72.4 % Ni, 79.6 % Co) while avoiding excessive energy input - no pressurized heating is required, as the temperature remains well below the boiling point of ethylene glycol (197.3 °C) - and minimizing solvent consumption. The moderate temperature is compatible with standard industrial equipment, and the low L/S ratio enhances metal concentration in the pregnant leach solution, reducing downstream processing costs. This combination of efficiency, safety, and resource economy makes the proposed DES-based route highly suitable for scalable and environmentally responsible valorization of asbestos waste.

Funding

This research was funded by the Science Committee of the Ministry of Science and Higher Education of the Republic of Kazakhstan (grantNo. AP22785975).

CRediT authorship contribution statement

Rustam Sharipov: Supervision, Project administration. **Assel Dagubayeva:** Writing – original draft. **Galymzhan Maldybayev:** Investigation, Data curation. **Mohamad Nasir Mohamad Ibrahim:** Writing – review & editing, Conceptualization. **Omirserik Baigenzhenov:** Writing – original draft, Methodology, Investigation. **Tiancheng Mu:** Writing – review & editing.

Declaration of competing interest

The authors declare that they have no known competing financial interests or personal relationships that could have appeared to influence the work reported in this paper.

Data availability

Data will be made available on request.

References

Abbott, A.P., Boothby, D., Capper, G., Davies, D.L., Rasheed, R.K., 2004. Deep eutectic solvents formed between choline chloride and carboxylic acids: versatile alternatives to ionic liquids. J. Am. Chem. Soc. 126 (29), 9142–9147. https://doi.org/10.1021/ja048266j.

Abdirashit, A., Kelamanov, B., Sariyev, O., Yessengaliyev, D., Abilberikova, A., Zhuniskaliyev, T., Kuatbay, Y., Naurazbayev, M., Nazargali, A., 2025. Study of nickel–chromium-containing ferroalloy production. Processes 13 (4), 1258. https://doi.org/10.3390/pr13041258.

Assylbekova, G., Sataev, M., Koshkarbayeva, S., Perminova, I., Abdurazova, P., 2023. Composite coatings: a comprehensive review of materials, methods and applications. Rep. NAS RK 348 (4), 148–168. https://doi.org/10.32014/2023.2518-1483.250.

Baigenzhenov, O.S., Chepushtanova, T.A., Altmyshbayeva, A.Z., Temirgali, I.A., Maldybayev, G., Sharipov, R.H., Altaibayev, B.T., Dagubayeva, A.T., 2024. Investigation of thermodynamic and kinetic regularities of asbestos waste leaching processes. Results Eng. 21, 102000. https://doi.org/10.1016/j.rineng.2024.102000.

Baigenzhenov, O.S., Kozlov, V.A., Luganov, V.A., Mishra, B., Shayahmetova, R.A., Aimbetova, I.O., 2015. Complex processing of wastes generated in chrysotile asbestos production. Miner. Process. Extr. Metall. Rev. 36 (4), 242–248. https://doi.org/10.1080/08827508.2014.955610.

Baigenzhenov, O., Khabiyev, A., Mishra, B., Aimbetova, I., Yulusov, S., Temirgali, I., Kuldeyev, Y., Korganbayeva, Z., 2022. Asbestos waste treatment - an effective process to selectively recover gold and other nonferrous metals. Recycling 7 (6), 85. https://doi.org/10.3390/recycling7060085.

Brown, M.E., 1997. The Prout-Tompkins rate equation in solid-state kinetics. Thermochim. Acta 300 (1–2), 93–106. https://doi.org/10.1016/S0040-6031(96)03119-X.

Calgaro, C.O., Tanabe, E.H., Bertuol, D.A., Silvas, F.P.C., Espinosa, D.C.R., Tenório, J.A. S., 2015. Leaching processes. In: Veit, H., Moura Bernardes, A. (Eds.), Electronic Waste. Topics in Mining, Metallurgy and Materials Engineering. Springer, Cham. https://doi.org/10.1007/978-3-319-15714-6_5.

Chu, L., Sun, H., Peng, T., Lu, H., Li, M., Zhang, Y., Luo, L., 2025. Selective extraction of Mg^{2+} from chrysotile asbestos tailings via ammonium sulfate roasting and water leaching: process optimization and mechanistic insights. J. Clean. Prod., 145773 https://doi.org/10.1016/j.jclepro.2025.145773.

Cimpoesu, F., Ferbinteanu, M., 2018. Coordination bonding: electronic structure and properties. Structural Chemistry. Springer, Cham. https://doi.org/10.1007/978-3-319-55875-2_6.

Deblonde, G.J.P., Chagnes, A., Cote, G., 2022. Recent advances in the chemistry of hydrometallurgical methods. Sep. Purif. Rev. 52 (3), 221–241. https://doi.org/10.1080/15422119.2022.2088389.

Delina, R.E.G., Perez, J.P.H., Stammeier, J.A., Bazarkina, E.F., Benning, L.G., 2024. Partitioning and mobility of chromium in iron-rich laterites from an optimized sequential extraction procedure. Environ. Sci. Technol. 58 (14), 6391–6401. https://doi.org/10.1021/acs.est.3c10774.

Gavrilă, C.C., Lateş, M.T., Grebenişan, G., 2024. Sustainable approach to metal coin canceling methods, using 3D modeling and finite element method analysis. Sustainability 16 (6), 2322. https://doi.org/10.3390/su16062322.

González-Gallardo, N., Cores, A., Marset, X., Guijarro, N., Guillena, G., Ramón, D.J., 2024. Unlocking the potential of deep eutectic solvents and ligand-to-metal charge transfer processes: a reusable iron-and-UV-based system for sustainable C−C bond formation. ChemSusChem 17 (24), e202400911. https://doi.org/10.1002/cssc.202400911.

Hartley, J.M., Ip, C.M., Forrest, G.C., Singh, K., Gurman, S.J., Ryder, K.S., Abbott, A.P., Frisch, G., 2014. EXAFS study into the speciation of metal salts dissolved in ionic liquids and deep eutectic solvents. Inorg. Chem. 53 (12), 6280–6288. https://doi.org/10.1021/ic500824r.

Ivanov, N.S., Malimbayev, M.S., Abilmagzhanov, A.Z., Kholkin, O.S., Adelbayev, I.Y., Brodskiy, A.R., 2022. Processing of oxidized nickel ores using sintering, roasting and leaching processes. Miner. Eng. 181, 107498. https://doi.org/10.1016/j.mineng.2022.107498.

Izquierdo, M., Querol, X., 2012. Leaching behaviour of elements from coal combustion fly ash: an overview. Int. J. Coal. Geol. 94, 54–66. https://doi.org/10.1016/j.coal.2011.10.006.

Kelamanov, B., Samuratov, Y., Akuov, A., Abdirashit, A., Burumbayev, A., Orynbassar, R., 2021. Research possibility of involvement Kazakhstani nickel ore in the metallurgical treatment. Metalurgija 60 (3–4), 313–316.

Kelamanov, B., Yessengaliyev, D., Sariev, O., Akuov, A., Samuratov, Y., Zhuniskaliyev, T., Kuatbay, Y., Mukhambetgaliyev, Y., Kolesnikova, O., Zhumatova, A., Karaidarova, Z., Abdirashit, A., 2024. Technological analysis of the production of nickel-containing composite materials. J. Compos. Sci. 8 (5), 179. https://doi.org/10.3390/jcs8050179.

Ketegenov, T., Kamunur, K., Mussapyrova, L., Batkal, A., Nadirov, R., 2024. Enhanced recovery of lithium and cobalt from spent lithium-ion batteries using ultrasound-assisted deep eutectic solvent leaching. Metals (Basel) 14 (9), 1052. https://doi.org/10.3390/met14091052.

Kurmanbayeva, I., Mentbayeva, A., Nurpeissova, A., Bakenov, Z., 2021. Advanced battery materials research at Nazarbayev University: review. Eurasian Chem.-Technol. J. 23 (3), 199–212. https://doi.org/10.18321/ectj1103.

Liu, Y., Lian, R., Wu, X., Dai, L., Ding, J., Wu, X., Van der Bruggen, B., 2023. Nickel recovery from electroplating sludge via bipolar membrane electrodialysis. J. Colloid Interface Sci. 637, 431–440. https://doi.org/10.1016/j.jcis.2023.01.113.

Macher, G.Z., Torma, A., Beke, D., 2025. Examining the environmental ramifications of asbestos fiber movement through the water–soil continuum: a review. Int. J. Environ. Res. Public Health 22 (4), 505. https://doi.org/10.3390/ijerph22040505.

Mamyrbayeva, K., Kuandykova, A., Chepushtanova, T., Merkibayev, Y., Brajendra, M., 2024. Studies of the extraction of nickel and cobalt from magnetic enrichment tailings. Eng. J. Satbayev Univ. 146 (5), 1–9. https://doi.org/10.51301/ejsu.2024.i5.01.

Massenova, A., Kalykberdiyev, M., Sass, A., Kenzin, N., Ussenov, A., Baiken, A., Rakhmetova, K., 2020. Catalytic technologies for solving environmental problems in the production of fuels and motor transport in Kazakhstan. Catalysts 10 (10), 1197. https://doi.org/10.3390/catal10101197.

Moskalyk, R.R., Alfantazi, A.M., 2002. Nickel sulphide smelting and electrorefining practice: a review. Miner. Process. Extr. Metall. Rev. 23 (3–4), 141–180. https://doi.org/10.1080/08827500306893.

Nadirov, R.K., Turan, M..D., Karamyrzayev, G.A., 2020. Copper Ammonia leaching from smelter slag. Int. J. Biol. Chem. 12 (2), 135–140. https://doi.org/10.26577/ijbch-2019-i2-18.

Osipov, P., Shayakhmetova, R., Murzalinov, D., Sagyndykov, A., Kali, A., Mukhametzhanova, A., Maldybayev, G., Mit, K., 2025. Electroplating composite coatings of nickel with dispersed WO_3 and MoO_3 on Al substrate to increase wear resistance. Materials (Basel) 18 (12), 2781. https://doi.org/10.3390/ma18122781.

Othman, Z.S., Hassan, N.H., Zubairi, S.I., 2015. Alcohol based-deep eutectic solvent (DES) as an alternative green additive to increase rotenone yield. In: AIP Conference Proceedings, 1678. AIP Publishing LLC, 050004. https://doi.org/10.1063/1.4931283.

Ray, H.S., Ray, S., 2018. Diffusion through product layer. Kinetics of Metallurgical Processes. Indian Institute of Metals Series. Springer, Singapore. https://doi.org/10.1007/978-981-13-0686-0_4.

Shayakhmetova, R.A., Mukhametzhanova, A.A., Akbayeva, D.N., Terlikbaeva, A.Z., Osipov, P.A., Alimzhanova, A.M., Zharmenov, A.A., 2024. Magnesium and silicon recovery from chrysotile asbestos waste of the deposit Zhitikara, Kazakhstan. Sci. Rep. 14 (1), 31866. https://doi.org/10.1038/s41598-024-83239-0.

Smith, E.L., Abbot, A.P., Ryder, K.S., 2014. Deep eutectic solvents (DESs) and their applications. Chem. Rev. 114 (21), 11060–11082. https://doi.org/10.1021/cr300162p.

Smith, R.J., Lewi, G.J., Yates, D.H., 2001. Development and application of nickel alloys in aerospace engineering. Aircr. Eng. Aerosp. Technol. 73 (2), 138–147. https://doi.org/10.1108/00022660110694995.

Tan, J., Huang, R., Li, K., Yan, X., Guo, L., Guo, Z., Zhang, W., Chai, L., 2024. Achieving high solid–Liquid ratio through competitive coordination towards efficient recovery of metals from spent batteries. Angew. Chem. Int. Ed. 16 (2), e202422313. https://doi.org/10.1002/anie.202422313.

Tian, L.I., Li, J., Hua, Y., 2010. Application of ionic liquids in hydrometallurgy of nonferrous metals. Trans. Nonferrous Met. Soc. China 20 (3), 513–520. https://doi.org/10.1016/S1003-6326(09)60171-0.

Tokpayev, R., Khavaza, T., Ibraimov, Z., Zhaksybay, B., Ciorita, A., Kishibayev, K., Zlobina, E., Nauryzbayev, M., 2025. Investigation and kinetic analysis of rare earth elements leaching: case study of the weathering crust of the Kundybay deposit (Northern Kazakhstan). Minerals 15 (5), 444. https://doi.org/10.3390/min15050444.

Yessengaziyev, A., Toishybek, A., Mukangaliyeva, A., Altaibayev, B., Smailov, K., Yersaiynova, A., Abdyldayev, N., 2025. Kinetics of acid leaching of niobium from man-made raw materials of titanium magnesium production: experimental research and modelling. Processes 13 (6), 1924. https://doi.org/10.3390/pr13061924.

Zante, G., Boltoeva, M., 2020. Review on hydrometallurgical recovery of metals with deep eutectic solvents. Sustain. Chem. 1 (3), 238–255. https://doi.org/10.3390/suschem1030016.